Vol. 41, No. 4 (2019) 613-621, DOI: 10.24874/ti.2019.41.04.13

Tribology in Industry

www.tribology.rs

RESEARCH

Wear Characteristics of Recycled Cast Al-6Si-3Cu Alloys

F.M. Mwema[a,b,*], J.O. Obiko[c], T. Leso[d], T.O. Mbuya[e], B.R. Mose[f], E.T. Akinlabi[b]

[a]*Department of Mechanical Engineering, Dedan Kimathi University of Technology, Nyeri, Kenya,*
[b]*Department of Mechanical Engineering Science, University of Johannesburg, Auckland Park, Johannesburg, South Africa,*
[c] *Department of Mining, Materials and Petroleum Engineering, Jomo Kenyatta University of Agriculture and Technology, Nairobi, Kenya,*
[d]*Department of Chemical, Metallurgy and Materials, Botswana International University of Science & Technology, Palapye,*
[e]*Department of Mechanical and Manufacturing Engineering, University of Nairobi, Nairobi, Kenya,*
[f]*Department of Mechanical Engineering, Jomo Kenyatta University of Agriculture and Technology, Nairobi, Kenya.*

Keywords:

Aluminium-silicon alloys
Intermetallic phases
Microstructure
Recycled
Wear

* Corresponding author:

Fredrick M. Mwema
E-mail: fredrick.mwema@dkut.ac.ke

Received: 30 May 2019
Revised: 12 September 2019
Accepted: 18 September 2019

A B S T R A C T

Recycling of Al-Si alloys for high integrity structural components for the automotive industry applications has gained attention in the recent times. In this article, scrap of cylinder heads containing 6.01%Si and 2.62%Cu were recycled by casting into four alloys invariants: base alloy (no alloying elements added), 0.02%Ca, 0.38%Fe and 0.9%Fe+0.45%Mn additions. The structural properties were analysed through optical and SEM/EDS microscopy, X-ray diffraction (XRD). The wear characteristics of the alloys were investigated using a multi-pass ball on the flat reciprocating method under a normal load of 30 N and velocity of 4 mm/s. The results showed delamination and adhesive wear as the predominant wear mechanisms for the recycled Al-Si alloys. The base and 0.02%Ca alloys exhibited the lowest coefficients of friction and rates of wear. A comparison of the wear data to the published data on primary alloys revealed that our secondary alloys have the potential for applications in the automotive industry.

1. INTRODUCTION

Cast Al-Si alloys especially those under 3xx.x and 4xx.x systems have found extensive applications in the automotive industry due to their excellent properties. Some of the beneficial attributes of these alloy systems include high strength-to-weight ratio, high fluidity (better cast-ability), excellent surface finish, better surface properties (corrosion and wear) and easier workability (deformation, joining, welding, etc.), high temperature strength and low thermal coefficient of expansion [1]. Early review work by Tenekedjiev and Gruzleski [2] offers detailed classifications and applications of Al-Si alloys. Since then, several studies have been conducted on improvement of Al-Si alloy for various automotive applications such as in engine parts, wheels, etc.[1] and as such the use of cast Al-Si alloy systems in the automotive industry has considerably increased [3]. The increase in utilisation of Al-Si alloys has led to an increase in scrap material and

therefore there is need for recycling to produce secondary Al-Si alloys for various applications [4].

Various works have been published on the production of secondary alloys from recycling of scrap Al-Si alloys [5] and it is generally agreed that impurities during re-melting and casting of these alloys are a major challenge. These impurities have a negative effect on the mechanical properties of the cast Al-Si components [6], [7]. Focus of most research on this subject has been to use alloying elements during casting to produce secondary alloys with comparable results to the primary alloys [8]–[10]. Wear is among the most significant property for automotive application of cast Al-Si alloys and various studies have been successfully conducted to understand the wear mechanisms and improve wear resistant of these alloys [11]–[14]. Despite this progress, there are very few publications reporting on the evaluation of wear performance of the secondary cast Al-Si alloys for automotive application. As such, this article evaluates the wear behaviour of cast secondary Al-Si-Cu invariants for automotive applications. The wear data obtained in this article has been compared to published data on wear of the primary cast Al-Si alloys.

2. EXPERIMENTAL

2.1 Materials

Scrap cylinder heads collected from different vendors in Nairobi City, Kenya were re-melt in a 70 Kg oil-fired graphite crucible and cast into 4 Kg conical moulds whose chemical compositions were determined as 6.01%Si, 2.62%Cu, 0.24%Mg, 0.28%Fe, 0.21%Mn, 0.02%Cr, 0.12%Zn, 0.02%Ni, 0.02%Ti, 0.01%Pb, 0.01%Sn. This material will be known as a base alloy in this paper. The ingots were then re-melt under an electric furnace at 750 °C in a cover flux. Three alloy variants containing 0.02%Ca (herein known as Ca-modified), 0.38%Fe (Fe- added) and 0.9%Fe+0.45%Mn (Fe-Mn added) were obtained by addition of respective granules and exhaustively stirred for chemistry homogenization. The addition of Ca into the alloy was meant to enhanced Si refinement as reported in literature [15], [16]. The addition of Fe and Mn influence both the microstructure and mechanical properties [17]. However, a proper ratio (2:1) of Fe to Mn must be used through mass balance (not described here) to achieve good microstructural evolution (). Furthermore, addition of transition elements such as Ni, Cr and Mn alter the morphology of the beta phases. Then, the melt was skimmed, degassed and then cast into 450 °C preheated permanent moulds [8], [18]. The samples were then heat treated in T6 temper, in which they were solution treated for 6 hours at 495 °C, water-quenched at 65 °C and artificially aged for 2 hours in a 170 °C air-circulated furnace. The samples were then sliced into 20 mm x 20 mm x 2 mm sizes for analyses.

2.2 Methods

Representative samples of the four alloys were hot-mounted, ground using SiC papers (#320-#1200), polished in diamond pastes (3 μm and 1 μm) and finely polished in colloidal silica. The microstructures were observed using optical (DP25 OLYMPUS) and scanning electron, SEM (Vega3 Tescan) microscopes. Elemental measurement was obtained by energy dispersive spectroscopy (EDS) system mounted within the Vega3 Tecan SEM facility.

XRD was used to undertake the qualitative analyses of the phases of the alloys using a diffractometer fitted with an anode source of CuKα (λ=1.5418Å) at 40 kV, 30 mA. A scan speed of 0.5 deg./min, scan step of 0.5 deg and a scan range of 5-90 deg were used in acquiring the XRD spectra. The samples for XRD test were ground of with #500 grit SiC paper to remove oxides.

The hardness tests were undertaken on the Vickers microhardness tester at a load of 15 Kgf, dwell time of 10 seconds and indenter approach rate of 50 μm/s. For each sample, 30 measurements were taken across their surfaces. The samples were prepared similarly to the microscopy samples.

Wear experiments were conducted under dry/unlubricated sliding multi-pass and reciprocating conditions against a steel ball of E52100 Alloy steel, grade 25 with a diameter of 6.350 mm (using a multifunctional tribometer, Rtec-instruments, San Jose, CA, USA). A scratch length of 5 mm and sliding velocity of 4 mm/s were chosen and each test was conducted for 42 minutes such that a total distance of 10 m was achieved. The ball was kept at a constant load of 30 N. The samples used in this test were ground using SiC papers of grit number #320 up to #1200 and then washed thoroughly in an

ultrasonic bath in water, then washed in acetone and finally dried in high-pressure hot air.

3. RESULTS AND DISCUSSIONS

3.1 Microstructure and Hardness

The optical and SEM/EDS microstructures of the recycled Al alloys are shown in Figs. 1 and 2. The base alloy was characterised by long eutectic silicon (grey) structures, interconnected plates of iron-based intermetallic phases and aluminium matrix (Figs. 1a and 2a). The EDS of this alloy in Fig. 2a confirms the interconnected plates as AlFeMnSiCu phases. The addition of 0.02%Ca (Ca-modified) results in modified silicon particles since Ca reduces the nucleation and growth of the Si during solidification and as such leading to formation of network of Si structures (Figs. 1b and 2b). Figure 1b further shows homogenized structure due to redistribution and spheroidization of the Si structures resulting from T6 treatment and artificial aging. A similar effect can be enhanced through addition of strontium. The addition of 0.38%Fe (Fe-added sample) reveal elongated, needle-like and spherical eutectic Si structures (Fig. 1c) and iron-based intermetallic phases (Fig. 2c). As shown in Figs. 1d and 2d, the addition of 0.9%Fe and 0.45%Mn results in formation of Chinese script phases (∝-AlFeMnSi) and eutectic Si particles. The Chinese scripts are well dispersed within the Al-matrix (Figs. 1a, 1c-1d). It is imperative to note that these alloys were all heat-treated (T6). After the T6 treatment, eutectic Si forms spheroids, i.e. Si-morphology changes from plate or sticks-like (in the plane of the cut they are needles or angular grains) to rod-like (in the plane of the cut they are round grains)-independently of the modification. Unmodified Si will have a round morphology after heat treatment (T6) too.

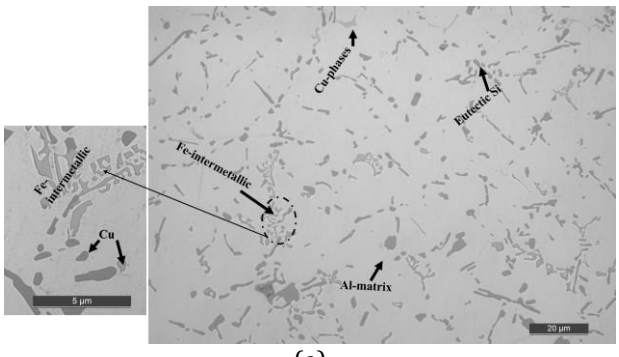

(a)

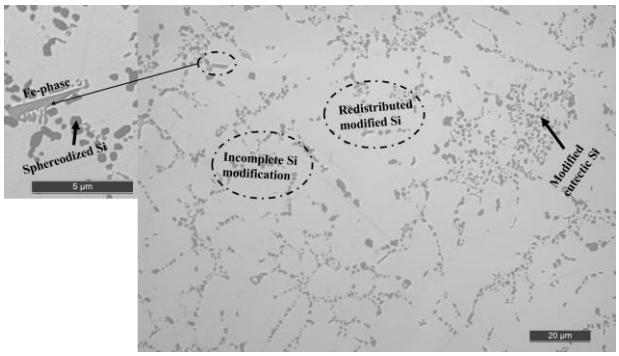

(b)

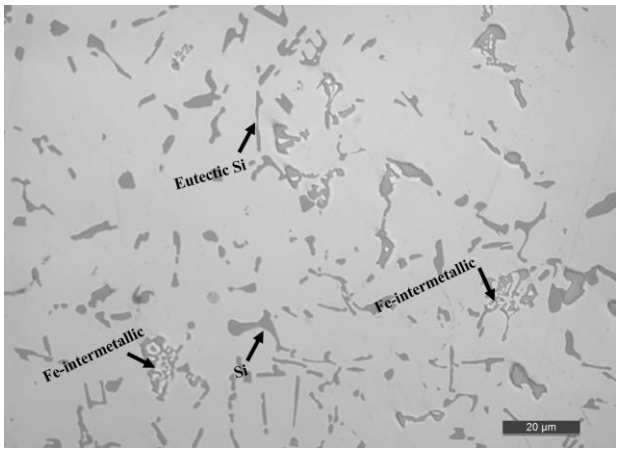

(c)

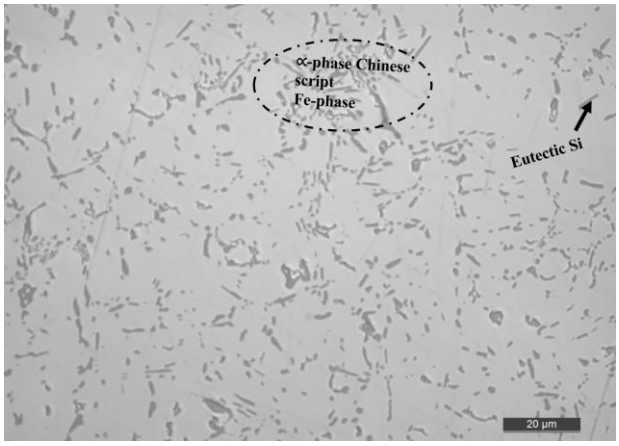

(d)

Fig. 1. Optical micrographs showing various morphologies of the secondary alloys (a) Base alloys (b) 0.02% Ca-modified (c) 0.38 % Fe-added (d) 0.9%Fe+0.45%Mn added.

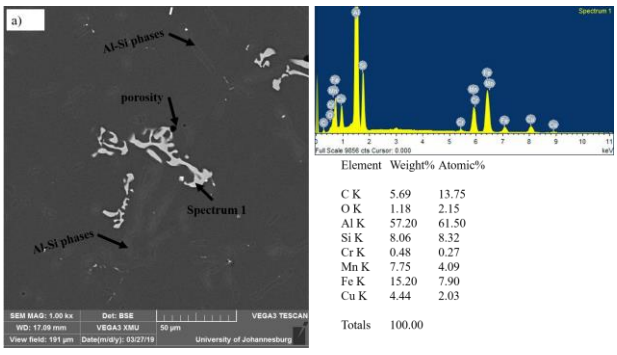

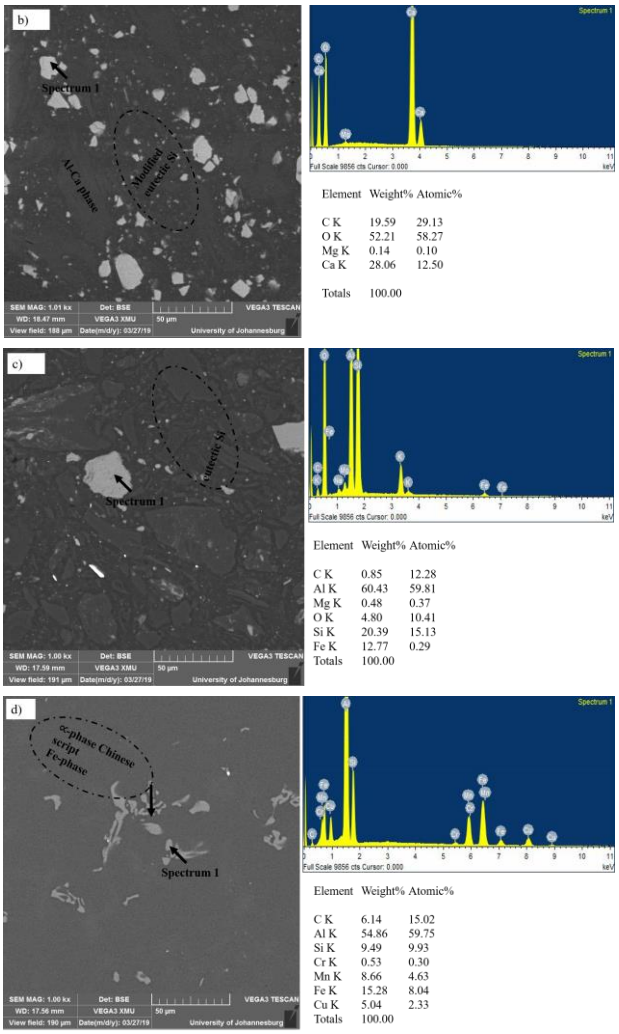

Fig. 2. SEM and EDS identification of the main intermetallic phases in each alloy (a) Base alloys (b) 0.02% Ca-modified (c) 0.38% Fe-added (d) 0.9%Fe+0.45%Mn added.

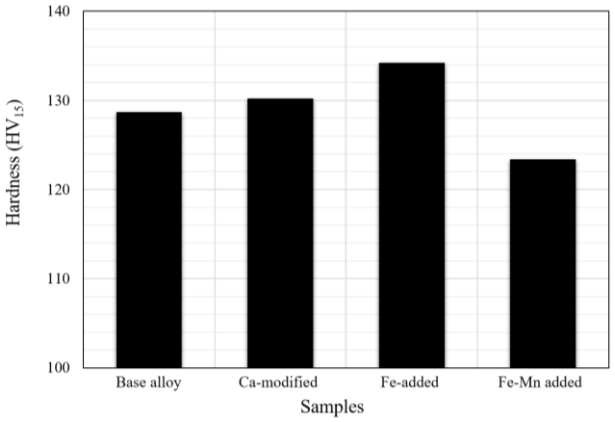

Fig. 3. Vickers hardness values of the secondary cast Al-Si-Cu alloys.

The alloys with 0.38%Fe (Fe-added) have the highest hardness values (134.2±0.41 HV), followed by the 0.02%Ca modified and the base alloys. The alloys containing 0.9%Fe+0.45%Mn have the lowest hardness values (123.4±1.48 HV) as shown in Fig. 3. The low hardness values in Fe-Mn added samples may be attributed to the presence of the Chinese script phases and further modification of Fe-bearing phases whereas the high hardness in Fe-added samples is due to the presence of spherical eutectic Si and AlFeSi intermetallic phases.

3.2 X-ray Diffraction (XRD)

The XRD spectra of the four alloys obtained in the 2θ range of 0-90˚ are shown in Fig. 4. The phases were identified using the International Centre for Diffraction Data (ICDD, PDF2010) database. The phases corresponding to the various peaks are indicated by color coding whose key is shown on the right-hand side of the graphs in Fig. 4.

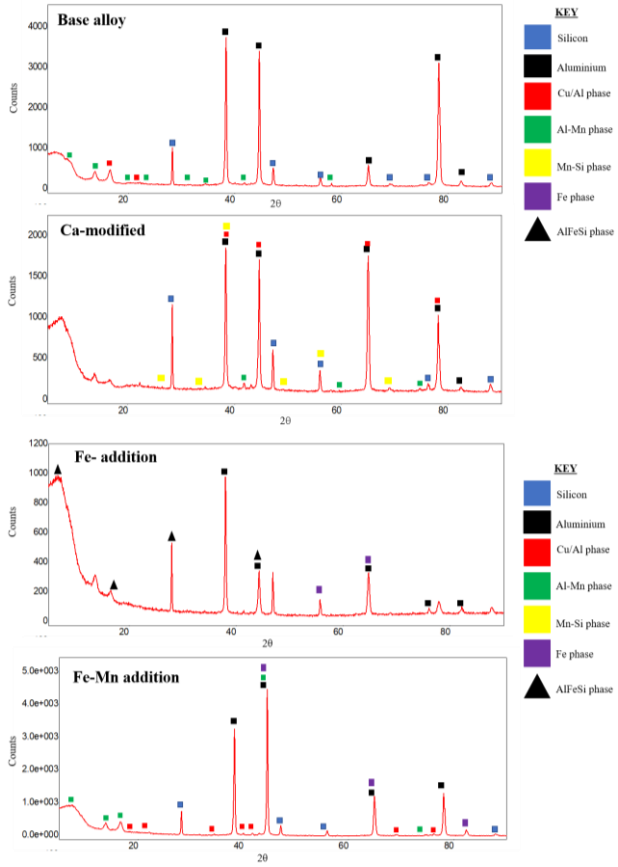

Fig. 4. X-ray diffraction patterns of the secondary cast Al-Si-Cu alloys.

As expected, the four alloys are dominated by Aluminium (database card: 00-005-0565) and Silicon (00-004-0787) phases. Other specific minor phases have also been identified. In the base alloy, cupalite (00-039-1371) and aluminium manganese, Al_{19} Mn_4 (03-065-3355) phases are present. In Ca-modified alloy, aluminium copper,

$Al_{0.99}Cu_{0.01}$ (01-074-5170), aluminium manganese, $Al_{0.55}Mn_{0.45}$ (00-039-1371) and manganese silicon, $Mn_{11}Si_{19}$ (03-065-2862) phases are present. In Fe-added alloy, aluminium iron silicide, $Al_{4.5}FeSi$ (01-087-0330), eta-$Cu_{3.17}Si$ (01-076-7859) and iron (01-077-7904) phases are present. Aluminium manganese, $Al_{78}Mn_{22}$ (00-039-1297), alpha-aluminium copper, $Al_{23}CuFe_4$ (03-065-7654) and iron (01-089-7194) were the minor phases present in Fe-Mn added samples.

3.3 Wear analysis

Figure 5 shows the representative wear tracks of the samples subjected to the reciprocating (multi-pass) ball-on-flat wear experiment. The results revealed a delamination and an adhesion as the predominant wear mechanisms. For the base alloy, there were grooves at the start of the loading of the ball followed by delamination and adhesion. The adhesion was observed at the sides whereas the delamination at the centre of the wear track of the base alloy. For the Ca-modified alloy, the wear was characterised by delamination along the sides of the wear track and adhesion transfer of the material to the centre and end of the wear track as shown in Fig. 5. The wear tracks for both Fe-added and Fe-Mn alloys were characterized by a high number of abrasion/longitudinal grooves through the track, delamination at the sides of the track and adhesion within the mid of the wear track. For both alloys, there were deep cuts of the ball indicating severe material removal. These observations imply that Fe- and Fe-Mn added alloys are more vulnerable to wear as further illustrated by the wear track profiles in Fig. 6. As shown in Fig. 6, measurements across the width of the wear track (shown as inset) provide insights into the depth of penetration of the steel ball onto the surface and hence extent of damage of the structure on sliding mechanical loads.

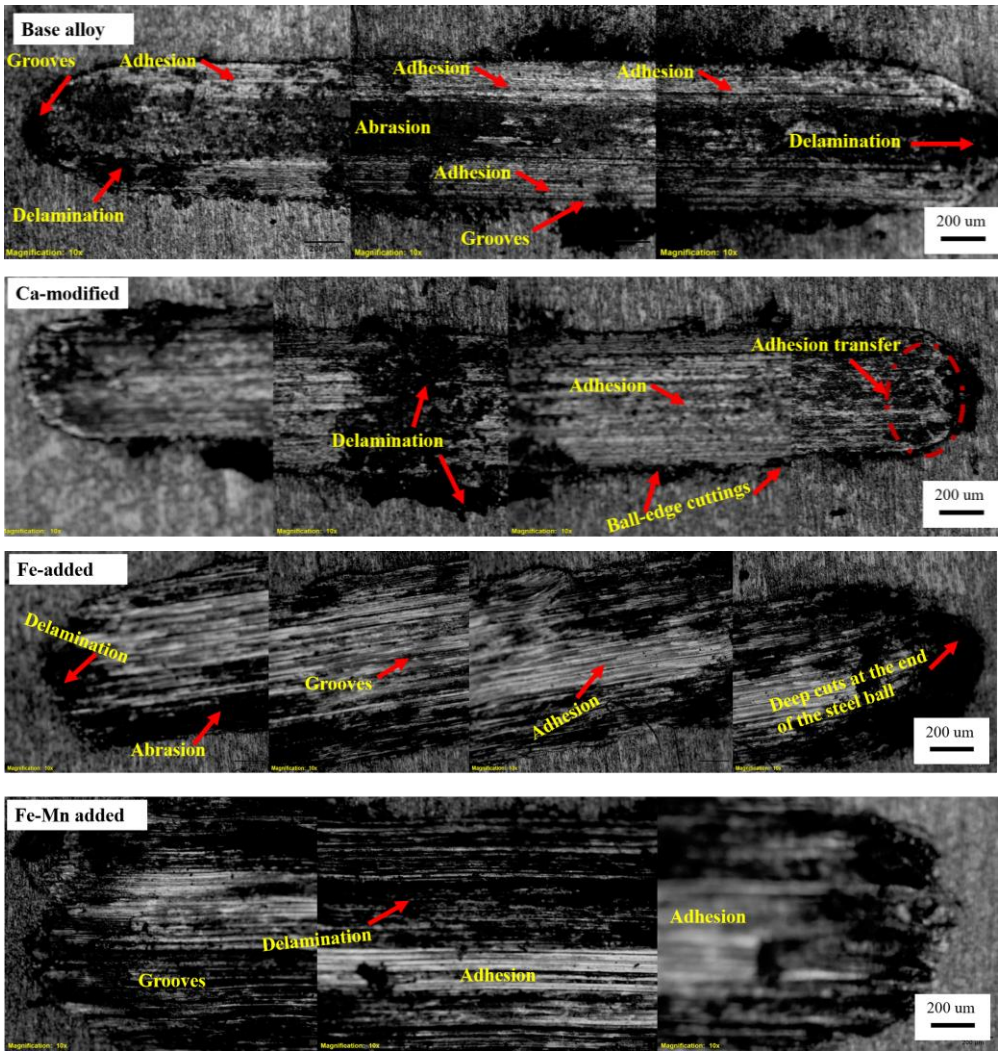

Fig. 5. Optical micrographs of the reconstructed wear tracks under dry sliding wear at 30 N.

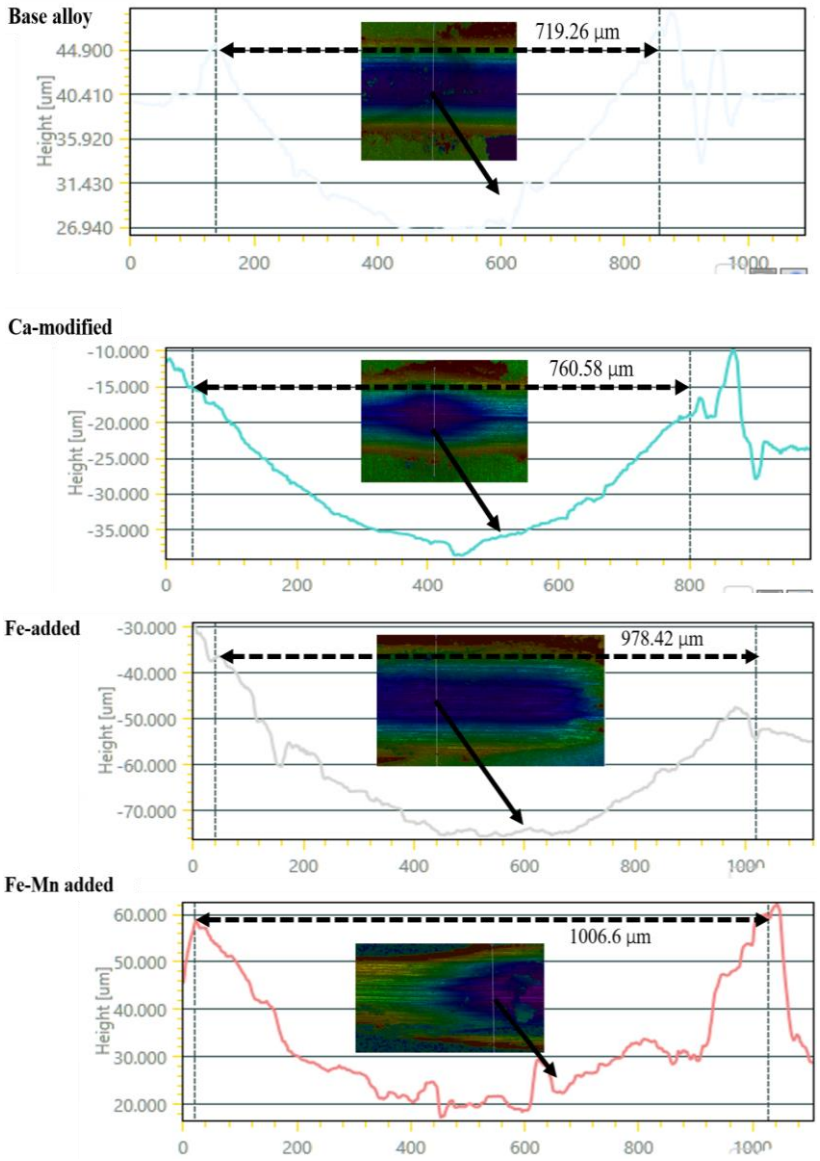

Fig. 6. Typical wear track profiles extracted across the width of wear track. The inset shows the stereo image of the wear track and illustrates the measurement of the height profile of the worn surfaces.

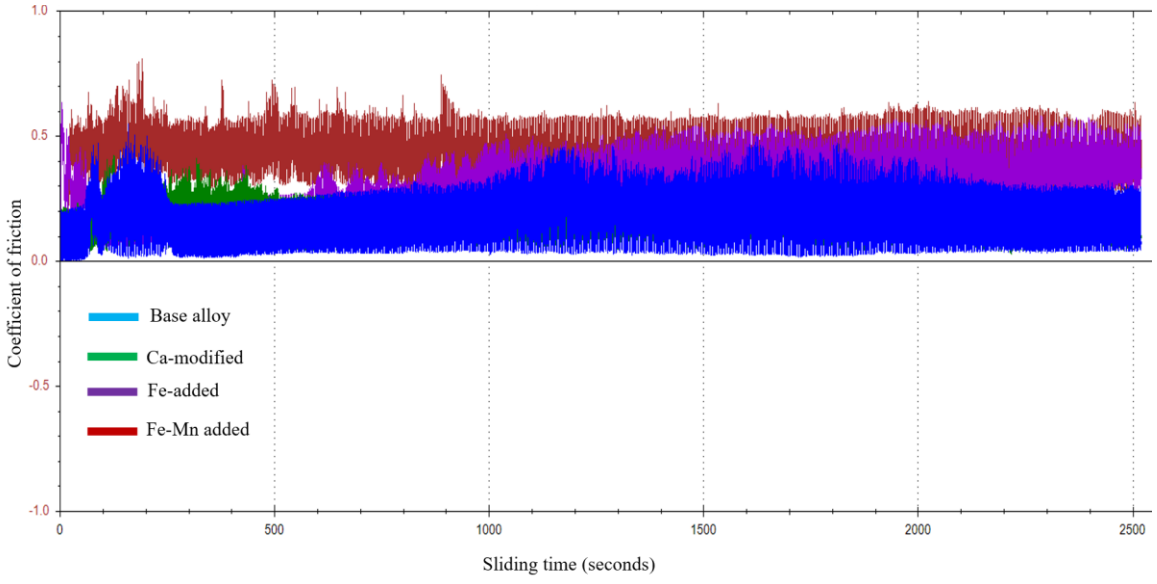

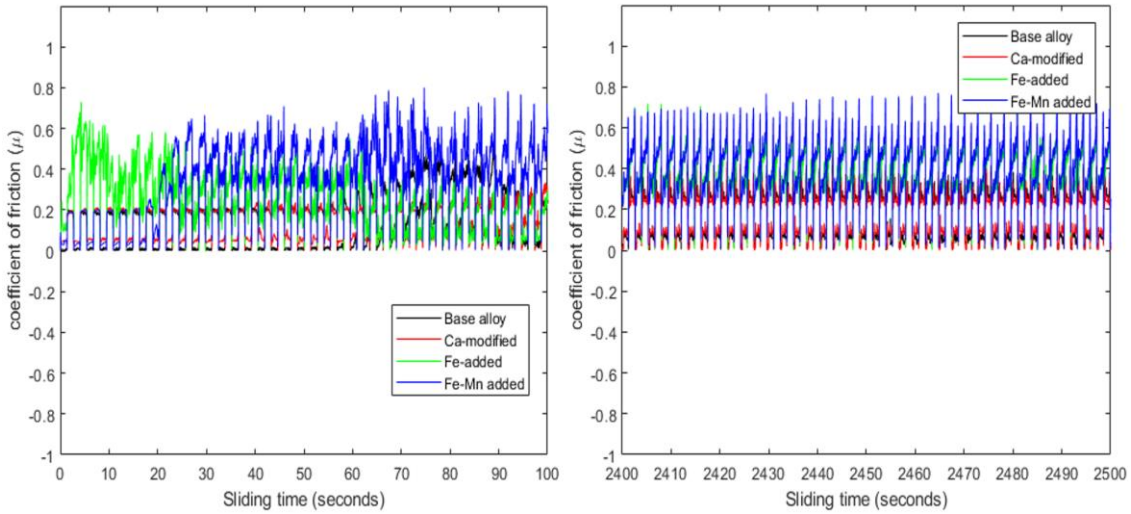

Fig. 7. Coefficient of friction (COF) as function of sliding time under dry wear conditions at 30 N. The plots for COF for the first and last 100 seconds are also shown.

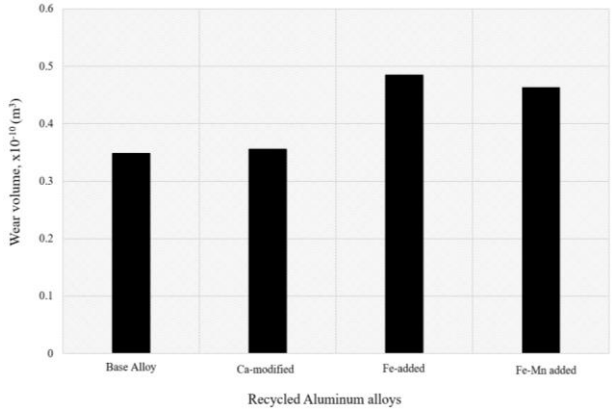

Fig. 8. Wear volume values of the secondary cast Al-Si-Cu alloys.

Figure 7 shows the plot of coefficient of friction (COF) against time (in seconds) for the alloys and it represents a typical behaviour for unlubricated reciprocating wear. Within the first 100 s of the experiments the COF was unstable and was characterised by nearly a square wave with the stability increasing with the time as illustrated. The average COFs were computed as 0.18±0.14, 0.16±0.10, 0.31±0.13 and 0.43±0.13 for base, Ca-added, Fe-added and Fe-Mn added alloys respectively. As expected, the alloys with the highest COFs (Fe- and Fe-Mn added) exhibit the highest wear volumes as shown in Fig. 8. The specific wear rates (Wsp = wear volume/(Total distance x Normal load)) were computed as $0.012x10^{-10}$, $0.012x10^{-10}$, $0.016x10^{-10}$ and $0.015x10^{-10}$ $m^3(Nm)^{-1}$ for base, Ca-added, Fe-added and Fe-Mn added alloys respectively.

The wear results show less correlation with the hardness values of the alloys indicating dominance of adhesion wear failure [13]. The base alloy and Ca-modified alloys exhibited the lowest wear rates whereas the Fe- and Fe-Mn added alloys have the highest wear rates. It also implies that Fe and Fe-Mn added alloys would be suitable for abrasive wear resistant rather than adhesion wear resistant. Samples with higher COF (Ca-added) exhibit higher failure in abrasive wear and lower failures in adhesive wear. These wear results can be related to the microstructural features observed through optical, SEM and XRD. For instance, addition of Fe- and Fe-Mn elements to the base alloys results in the formation of intermetallic iron-bearing phases such as those identified via EDS and XRD techniques. These iron-based phases breakdown to create third body abraders and hence accelerating material removal through abrasive wear. This is the reason for very many abrasive grooves observed in the wear tracks of these alloys as shown in Fig. 5. The contribution of silicon content and its morphology in Al-Si alloys to wear behaviour is an important consideration in explaining these results. Generally, mechanical properties of Al-Si alloys depend more on the shape, size and distribution of Si particles rather than the composition of the silicon in the alloy [11]. Fine, spherical and uniformly distributed Si particles in the matrix enhance ductility and strength. Long and acicular silicon particles, on the other hand, enhance high strength and lower ductility, fatigue and impact strengths [11]. Ca-added alloy exhibited the best wear resistance, which may be attributed to the modification of silicon morphology (through addition of calcium during solidification), which enhances high

ductility and relatively high strength. The presence of faceted and acicular silicon in Fe- and Fe-Mn added alloys can be attributed to high wear rates since there is a higher likelihood of crack nucleation at the silicon particle-aluminium matrix. Additionally, the heat treatment undertaken on the alloys enhances spheroidization of silicon particles, which was clearly observed on base alloy (through necking of the Si to form spheroids) and Ca-added alloy. Spheroidization reduces the stress concentration at the matrix-particle interface and therefore enhances wear resistance.

These wear results are comparable to published data on wear of Al-Si alloys. A study on sliding wear behaviour of hypereutectic Al-Si alloys with silicon composition ranging between 17wt% and 30.3wt% was undertaken using AISI Grade 316 ball of diameter 5 mm [13]. The values of the specific wear rates ranged between 0.07 and 0.11 $m^3(Nm)^{-1}$, which were quite higher than those reported in this study. In another study [12], the coefficient of friction of hypereutectic Al-14wt%Si-Cu alloy subjected under dry sliding pin-on-disk wear was reported in the range of 0.15-0.6, which are comparable to those computed in this article. Comparable results were also reported for Al-17Si-Cu alloys [14], Al-57.5Si-Cu-Mg [19], LM30-sillimanite composite [20] and among others.

4. CONCLUSION

Based on the experiments and analyses presented in this paper, the following conclusions have been drawn:

- The specific wear rates and coefficients of friction of the four secondary alloys (hypoeutectic) in this paper present similar behaviour of primary Al-Si alloys under dry wear conditions. As such, these alloys are potential candidates for application in areas where primary Al-Si alloys are used such as in production of automotive parts.
- Lower specific wear rates and friction coefficients were observed on base and 0.02%Ca modified alloys. The 0.38%Fe containing alloy exhibited the highest specific wear rate whereas 0.9%Fe+0.45%Mn alloy had the highest value of coefficient of friction.
- The wear mechanisms for the alloys was mainly by delamination and adhesive failure. For alloys containing Fe alloying element abrasive grooves indicating abrasive wear mechanisms were also observed besides the delamination and adhesive mechanisms.

Acknowledgement

Ghebrezghi T. Zeru is highly acknowledged for collecting and supplying the scrap cylinder head aluminium-silicon scrap.

REFERENCES

[1] T.O. Mbuya, B.O. Odera, S.P. Ng'ang'a, *Influence of iron on castability and properties of aluminium silicon alloys: Literature review*, International Journal of Cast Metals Research, vol. 16, iss. 5, pp. 451–465, 2003, doi: 10.1080/13640461.2003.11819622

[2] N. Tenekedjiev, J.E. Guzleski, *Hypereutectic Aluminium-Silicon Casting Alloys—A Review*, Cast Metals, vol. 3, iss. 2, pp. 96–105, 1990, doi: 10.1080/09534962.1990.11819026

[3] M. Javidani, D. Larouche, *Application of cast Al–Si alloys in internal combustion engine components*, International Material Reviews, vol. 59, iss. 3, pp. 132–158, 2014, doi: 10.1179/1743280413Y.0000000027

[4] E. Velasco, J. Nino, *Recycling of aluminium scrap for secondary Al-Si alloys*, Waste Management & Research, vol. 29, iss. 7, pp. 686–693, 2011, doi: 10.1177/0734242X10381413

[5] E. Tillov, M. Chalupov, L. Hurtalov, *Evolution of Phases in a Recycled Al-Si Cast Alloy During Solution Treatment*, in D. V. Kazmiruk (Ed): Scanning Electron Microscopy, IntechOpen Limited, United Kingdom, pp. 411–436, 2012.

[6] M.N. Ervina Efzan, H.J. Kong, C.K. Kok, *Review: Effect of Alloying Element on Al-Si Alloys*, Advanced Material Researc, vol. 845, pp. 355–359, 2013, doi: 10.4028/www.scientific.net/AMR.845.355

[7] W.S. Ebhota, T.-C. Jen, *Intermetallics Formation and Their Effect on Mechanical Properties of Al-Si-X Alloys*, in Mahmood Aliofkhazraei (ED): Intermetallic Compounds - Formation and Applications, IntechOpen Limited, United Kingdom, pp. 1–28, 2018, doi: 10.5772/intechopen.73188

[8] B.R. Mose, S.M. Maranga, T.O. Mbuya, *Effect of Minor Elements on the Fluidity of Secondary*

LM25 and LM27-Type Cast Alloys, Transcactions of American Foundry Society, vol. 117, pp. 93–101, 2009.

[9] L. Hurtalova, E. Tillová, M. Chalupová, E. Duriníková, *Effect of chemical composition of secondary Al-Si cast alloy on intermetallic phases*, Machines, Technologies, Materials, vol. 3, pp. 23–26, 2012.

[10] D. Bösch, S. Pogatscher, M. Hummel, W. Fragner, P.J. Uggowitzer, M. Göken, H.W. Höppel, *Secondary Al-Si-Mg High-pressure Die Casting Alloys with Enhanced Ductility*, Metallurgical and Materials Transactions A, vol. 46, iss. 3, pp. 1035–1045, 2015, doi: 10.1007/s11661-014-2700-8

[11] D.K. Dwivedi, *Adhesive wear behaviour of cast aluminium-silicon alloys: Overview*, Materials & Design, vol. 31, iss. 5, pp. 2517–2531, 2010, doi: 10.1016/j.matdes.2009.11.038

[12] D.E. Lozano, R.D. Mercado-Solis, A.J. Perez, J. Talamantes, F. Morales, M.A.L. Hernandez-Rodriguez, *Tribological behaviour of cast hypereutectic Al-Si-Cu alloy subjected to sliding wear*, Wear, vol. 267, iss. 1–4, pp. 545–549, 2009, doi: 10.1016/j.wear.2008.12.112

[13] F. Alshmri, H.V. Atkinson, S.V. Hainsworth, C. Haidon, S.D.A. Lawes, *Dry sliding wear of aluminium-high silicon hypereutectic alloys*, Wear, vol. 313, iss. 1–2, pp. 106–116, 2014, doi: 10.1016/j.wear.2014.02.010

[14] B. Hazra, P. Baranwal, S. Bera, B.K. Show, *Improvement in dry sliding wear resistance of Al-17Si-5Cu alloy after an enhanced heat treatment process*, Transactions of Nonferrous Metals Society of China, vol. 28, iss. 9, pp. 1705–1713, 2018, doi: 10.1016/S1003-6326(18)64814-9

[15] X. Jiao, C.-f. Liu, J. Wang, Z.-p. Guo, J.-y. Wang, Z.-m. Wang, J.-m. Gao, S.-m. Xiong, *Effect of Ca addition on solidification microstructure of hypoeutectic Al-Si casting alloys*, China Foundry, vol. 16, iss. 3, pp. 153–160, 2019, doi: 10.1007/s41230-019-9014-9

[16] K. Al-Helal, Y. Wang, I. Stone, Z.Y. Fan, *Effect of Ca Level on the Formation of Silicon Phases during Solidification of Hypereutectic Al-Si Alloys*, Materials Science Forum, vol. 765, pp. 117–122, 2013, doi: 10.4028/www.scientific.net/MSF.765.117

[17] S. Ji, W. Yang, F. Gao, D. Watson, Z. Fan, *Effect of iron on the microstructure and mechanical property of Al–Mg–Si–Mn and Al–Mg–Si diecast alloys*, Materials Science and Engineering: A, vol. 564, pp. 130–139, 2013, doi: 10.1016/j.msea.2012.11.095

[18] F.M. Mwema, *Microstructural and Microhardness Characterization of Primary and Recycled Cast Al-Si Piston Alloys Processed by High-Pressure Torsion*, Master's Thesis, Department of Mechanical Engineering, Jomo Kenyatta University of Agriculture & Technology, Nairobi, 2015.

[19] M.L. Rahaman, L. Zhang, *An investigation into the friction and wear mechanisms of aluminium high silicon alloy under contact sliding*, Wear, vol. 376–377, pp. 940–946, 2017, doi: 10.1016/j.wear.2016.10.026

[20] S. Sharma, T. Nanda, O.P. Pandey, *Investigation of T4 and T6 heat treatment on the wear properties of sillimanite reinforced LM30 aluminium alloy composites*, Wear, vol. 426–427, pp. 27–36, 2019, doi: 10.1016/j.wear.2018.12.065